J Arid Land (2019) 11(5): 664–673
https://doi.org/10.1007/s40333-019-0105-7

Science Press Springer-Verlag

Reinvestigation of the scaling law of the windblown sand launch velocity with a wind tunnel experiment

ZHANG Yang[1*], LI Min[1], WANG Yuan[1], YANG Bin[2]

[1] Department of Fluid Machinery and Engineering, Xi'an Jiaotong University, Xi'an 710049, China;
[2] School of Chemical Engineering, Northwest University, Xi'an 710069, China

Abstract: Windblown sand transport is a leading factor in the geophysical evolution of arid and semi-arid regions. The evolution speed is usually indicated by the sand transport rate that is a function of launch velocity of sand particle, which has been investigated by the experimental measurement and numerical simulation. However, the obtained results in literatures are inconsistent. Some researchers have discovered a relation between average launch velocity and wind shear velocity, while some other researchers have suggested that average launch velocity is independent of wind shear velocity. The inconsistence of launch velocity leads to a controversy in the scaling law of the sand transport rate in the windblown case. On the contrary, in subaqueous case, the scaling law of the sand transport rate has been widely accepted as a cubic function of fluid shear velocity. In order to explain the debates surrounding the windblown case and the difference between windblown and subaquatic cases, this study reinvestigates the scaling law of the vertical launch velocity of windblown transported sand particles by using a dimensional analysis in consideration of the compatibility of the characteristic time of sand particle motion and that of air flow. Then a wind tunnel experiment is conducted to confirm the revisited scaling law, where the sand particle motion pictures are recorded by a high-speed camera and then the launch velocity is solved by the particle tracking velocimetry. By incorporating the results of dimensional analysis and wind tunnel experiment, it can be concluded that, the ratio of saltons number to reptons number determines the scaling law of sand particle launch velocity and that of sand transport rate, and using this ratio is able to explain the discrepancies among the classical models of steady sand transport. Moreover, the resulting scaling law can explain the sand sieving phenomenon: a greater fraction of large grains is observed as the distance to the wind tunnel entrance becomes larger.

Keywords: windblown sand transport; scaling law; launch velocity; dimensional analysis; wind tunnel

Citation: ZHANG Yang, LI Min, WANG Yuan, YANG Bin. 2019. Reinvestigation of the scaling law of the windblown sand launch velocity with a wind tunnel experiment. Journal of Arid Land, 11(5): 664–673. https://doi.org/10.1007/s40333-019-0105-7

1 Introduction

Windblown sand transport is a leading factor in the geophysical evolution of arid and semi-arid regions (Bagnold, 1941; Kok et al., 2012; Burr et al., 2015). The launch velocity of sand particle is important to quantify the windblown sand transport, to which the experimental measurement is one of the main researching approaches. However, the obtained experimental results are inconsistent. Some researchers have discovered a relation between average launch velocity and wind shear

*Corresponding author: ZHANG Yang (E-mail: zhangyang1899@mail.xjtu.edu.cn)
Received 2018-07-26; revised 2019-04-02; accepted 2019-05-27

velocity (Owen, 1964; Bagnold, 1973; Anderson and Hallet, 1986; McEwan and Willetts, 1993), while some other researchers have suggested that average launch velocity is independent of wind shear velocity (Namikas, 2003; Rasmussen and Sørensen, 2008; Creyssels et al., 2009; Martin and Kok, 2017). Numerical simulations conducted by Feng et al. (2009) demonstrated that over an erodible sand bed, average launch velocity is independent of wind shear velocity for low wind velocities, but increases with wind shear velocity for high wind velocities. Ho et al. (2011) fed sand particles at the upwind end of a wind tunnel and experimentally studied the influence of sand bed configuration on sand motion. Their results demonstrated that average launch velocity is independent of wind shear velocity over erodible sand beds; however, average launch velocity depends on wind shear velocity over non-erodible sand beds. The debate on launch velocity has been extended to the dependence of steady sand transport rate on wind shear velocity (Martin and Kok, 2017), which has been suggested to be cubic (Bagnold, 1941; Kind, 1976), quadratic (Creyssels et al., 2009; Martin and Kok, 2017) or even variational (Sauermann et al., 2001; Durán et al., 2011; Ho et al., 2011). In contrast to the windblown case, the dependence of steady sand transport rate on fluid shear velocity has been determined to be cubic in the subaquatic case (Martin and Kok, 2017; Wu et al., 2018).

The horizontal component of launch velocity is expected to scale with the square root of the product of gravitational acceleration and average sand particle diameter according to the balance among the forces acting on sand particles. So, it is the vertical component of launch velocity that must be responsible for the controversies among the models discussed above. The purpose of this paper is to provide a unified interpretation for the controversies based on the scaling law for the vertical component of sand launch velocity. The present work is divided to three parts. Firstly, a simple dimensional analysis is carried out to revisit the scaling law for vertical launch velocity and steady sand transport rate. Secondly, a wind tunnel experiment on windblown sand flow is conducted to test the scaling law. Thirdly, an analysis based on the revisited scaling law is proposed to explain the controversies among the classical models.

2 Scaling law revisited by using a dimensional analysis

The definition of the focus point has to be revisited in the first place. As shown in Figure 1, the focus point is the locus where wind velocity is independent of wind shear (friction) velocity (u_f) (Bagnold, 1941; Owen, 1964). Sand motion below the focus point is almost independent of wind strength and that above the focus point is affected by wind strength. Therefore, it is reasonable to distinguish reptation and saltation based on the observed particle trajectory height. Here sand particles that never move above the focus point are called reptons and those that can go above the focus point are called saltons (Bagnold, 1941; Ho et al., 2014). In subaqueous cases, most sand particles are in suspension, which literally move above the focus point. In the present paper, such suspending particles are also named saltons for the sake of a unified framework. These definitions are considered the resultant expressions of the original definitions, in which the saltons are those driven by wind and impact on the sand bed, and reptons are those splashed by saltons (Antdrotti et al., 2002).

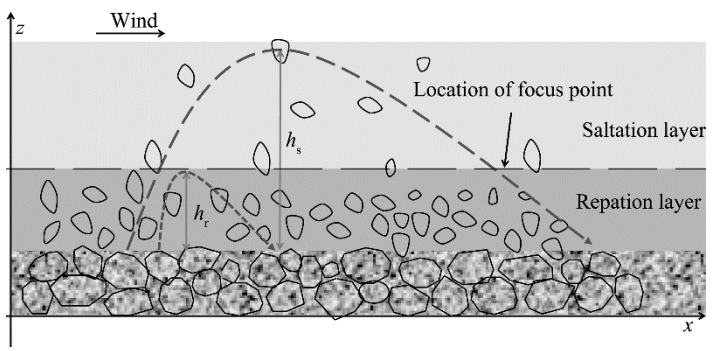

Fig. 1 Transport layer of windblown sand particles. h_r and h_s are the characteristic hop heights (m) of reptons and saltons, respectively.

Suppose the characteristic times of the sand motion and macroscopic structure of the air flow must have the same order of magnitude; otherwise, no interaction would exist between the two motions. This is similar to the correlation between the mean flow and the largest eddy in the turbulence (Tennekes and Lumley, 1972). As a result, we have:

$$v / g = c_0 (\partial U / \partial z)^{-1}, \tag{1}$$

where v is the vertical launch velocity of sand particles (m/s); g is the acceleration of gravity (m/s^2); c_0 is a coefficient of order unity; U is the horizontal wind velocity (m/s); and z is the vertical coordinate (m). v/g represents the characteristic time of sand particle motion (s), $(\partial U/\partial z)^{-1}$ is the reciprocal of the velocity gradient and accounts for the characteristic time of the air flow that interacts with sand particles.

The wind velocity at the focus point is proportional to $(gd)^{1/2}$, and it is independent of u_f (friction velocity) below the focus point (Ho et al., 2014). Let's define that the subscripts 's' and 'r' refer to the parameters of saltons and reptons, respectively. Then in the reptation layer, the characteristic wind velocity U_r scales with $(gd)^{1/2}$, and the characteristic length is the hop height of the reptons, h_r, which scales with $v_r^2/(2g)$. Following Equation 1, the vertical launch velocity (v_r) of reptons is:

$$v_r \sim g(h_r / U_r) \sim v_r^2 / (2(gd)^{1/2}). \tag{2}$$

So one can obtain $v_r=2c_r(gd)^{1/2}$, where "~" means that the scaling factor between the two sides is within a magnitude of five times (Tennekes and Lumley, 1972). That is to say, c_r is a coefficient that ranges from 0.2 to 5.0.

In the saltation layer, as shown in Figure 1, the characteristic length is the hop height of the saltons h_s, which scales with $v_s^2/(2g)$. The characteristic wind velocity U_s scales with the effective wind shear velocity (u_f–u_{ft}), where u_{ft} is the threshold wind shear velocity above which sand particles can be set in motion. According to Equation 1, the v_s of the saltons is:

$$v_s \sim g(h_s / U_s) \sim v_s^2 / (2(u_f - u_{ft})). \tag{3}$$

So $v_s=2c_s(u_f–u_{ft})$. Similarly, c_s is a coefficient ranging from 0.2 to 5.0. As a result, the hop heights for reptons and saltons can be expressed as:

$$\begin{aligned} h_r &= 2c_r^2 d \\ h_s &= 2c_s^2 (u_f - u_{ft})^2 / g \end{aligned}. \tag{4}$$

The hop length is $l=u_m(2v/g)$, where u_m is the average horizontal velocity (m/s) of sand particles. Although the characteristic horizontal velocity of sand is unknown, moving sand is accelerated by wind in the horizontal direction. Therefore, u_m is roughly proportional to the characteristic wind velocity. Then one obtains:

$$\begin{aligned} l_r &\propto U_r(2v_r / g) \propto d \\ l_s &\propto U_s(2v_s / g) \propto (u_f - u_{ft})^2 / g \end{aligned}, \tag{5}$$

where l_r and l_s are the hop lengths (m) of reptons and saltons, respectively; and $\propto$ means that the left side is proportional to the right side, and the range of the scaling factor is uncertain. Comparison of Equations 4 and 5 shows that the ratio of hop length to hop height is constant for reptons and saltons, which is consistent with experimental results (Zhang et al., 2007; Ho et al., 2011, 2014). On the basis of momentum conservation, the steady sand transport rate can be obtained as (Sørensen, 2004):

$$q = l_m(\tau - \tau_t) / (u_\downarrow - u_\uparrow), \tag{6}$$

where l_m is the average hop length (m); τ is the shear stress ($\tau=\rho u_f^2$ with ρ=1.25 kg/m^3 being the air density); τ_t is the threshold shear stress ($\tau_t=\rho u_{ft}^2$); $u_\uparrow$ and $u_\downarrow$ are the average horizontal velocities of sand particles taking off from and landing on the sand bed, respectively; and $(u_\downarrow$–$u_\uparrow)$ is roughly proportional to the characteristic wind velocity as $(u_\downarrow$–$u_\uparrow)\propto(gd)^{1/2}$ if the majority of the moving particles are reptons, and as $(u_\downarrow$–$u_\uparrow)\propto(u_f$–$u_{ft})$ if the majority of the moving particles are saltons. Combination with Equation 5 yields:

$$q_r \propto \rho(u_f^2 - u_{ft}^2)(d/g)^{1/2}, \tag{7}$$

$$q_s \propto \rho(u_f - u_{ft})(u_f^2 - u_{ft}^2)/g. \tag{8}$$

3 Wind tunnel experiment

Equations 4–8 are derived by supposing that vertical launch velocity scales with $(gd)^{1/2}$ for reptons and scales with (u_f-u_{ft}) for saltons. A wind tunnel experiment is introduced to testify this conclusion.

The experiment is conducted at the Laboratory of Windblown Sand Dynamics, Xi'an Jiaotong University, China. As shown in Figure 2a, such laser based configuration has been widely used in the measurement of windblown sand transport (Zhang et al., 2007, 2008; Wang et al., 2009; Yang et al., 2009; Kang, 2012; Zhang et al., 2014; O'Brien and McKenna Neuman, 2016, 2018). The test section of the wind tunnel has a size of 6.75 m^x×0.72 m^y×0.60 m^z, with x denoting the mainstream direction, y the transverse direction and z the vertical direction. The wind is sent out by two abreast air blowers. In order to fully mix the two air jets and to smooth the turbulence caused by air blowers, a distance of 5.0 m, which is paved with roughness elements, is set between the wind tunnel entrance and the upstream edge of sand bed. Thus the sand bed with a size of 1.0 m^x×0.2 m^y×0.01 m^z is placed 5.0 m downstream of the wind tunnel entrance. A high-speed digital camera (FASTCAM-APX 120K, Photron, Japan) is placed at the side of wind tunnel, with its view line perpendicular to the side wall plane. The frame rate of the digital camera is 2000 Hz, the exposure time is 1/3000 s, and the resolution is 1024 pixel×572 pixel. The observation region is 138.4 mm^x×69.2 mm^z, which is illuminated by a sheet laser (Mini-YAG, 100 mJ). The diameter range of the three sand samples in the present experiment are 100–125 μm with a density of 2702.8 kg/m^3, 200–300 μm with a density of 2650.0 kg/m^3 and 300–500 μm with a density of 2650.0 kg/m^3. One of the recorded particle images in the present experiment is shown in Figure 2b. The moderate sand particle concentration (especially above the focus point) allows for the Lagrangian particle detection to catch the particle trajectory. Firstly, the dynamic threshold scheme (Ohmi and Li, 2000; Zhang et al., 2016) is used to realize the image segmentation and the recognition of moving particles. On a grey-scale particle image, a small window is built and shifted, and a local grey-scale threshold in this window is continuously computed and applied to distinguish the particle image of multiple grey-scale levels from background (Fig. 2c). This operation is also called the reconstruction of particle image. Secondly, after the operation of Voronoi diagram on a reconstructed particle image sequence, each particle across the sequence corresponds to a unique Voronoi polygon, so each particle can be tracked across the frame based on the geometric stability of such polygon (Zhang et al., 2015, 2016). As a helper method, a central-differential schemed static background elimination method called the "non-zero subtraction algorithm" is applied to extract the moving sand particles near the sand bed (Zhang et al., 2016). Nevertheless, those touching closely the sand bed are difficult to extract due to the over exposed reflection at the sand bed. The result is satisfactory as shown in Figure 2d.

The streamwise mean velocity profile $U=U(z)$ is measured by an array of hot-wire probes (55R49, Dantec Inc., Denmark), which are the nikel-plating type and located downstream of the observation region. Before the measurement, the sand bed was fixed by spraying water. The reference wind velocity U_0 is measured 0.26 m above the sand bed surface. As shown in Figure 3, the profile is well-fitted by the logarithmic law.

The wind shear velocities are calculated from the wind velocity profiles, which are 0.23 and 0.30 m/s for the two cases of 100–125 μm sand, 0.40 and 0.46 m/s for the two cases of 200–300 μm sand, and 0.41 and 0.51 m/s for the two cases of 300–500 μm sand, respectively. The particle Reynolds number Re are 1.7136 and 2.2351 for 100–125 μm sand, 6.6225 and 7.6159 for 200–300 μm sand, and 10.8609 and 13.5099 for 300–500 μm sand. The characteristic length and velocity are sand diameter and wind shear velocity. In another independent set of tests, the threshold velocity of sand motion for the above three sand samples is determined by using the technique shown in Figure 2d, and the corresponding threshold wind velocity profile is measured and used to calculate

u_{ft}. The results are 0.15, 0.23 and 0.29 m/s for the samples corresponding to the diameter ranges of 100–125, 200–300 and 300–500 μm, respectively, agreeing well with the classical model $u_{ft}=0.1[gd(\rho_s-\rho)/\rho]^{1/2}$, where ρ=1.25 kg/m^3 is the air density.

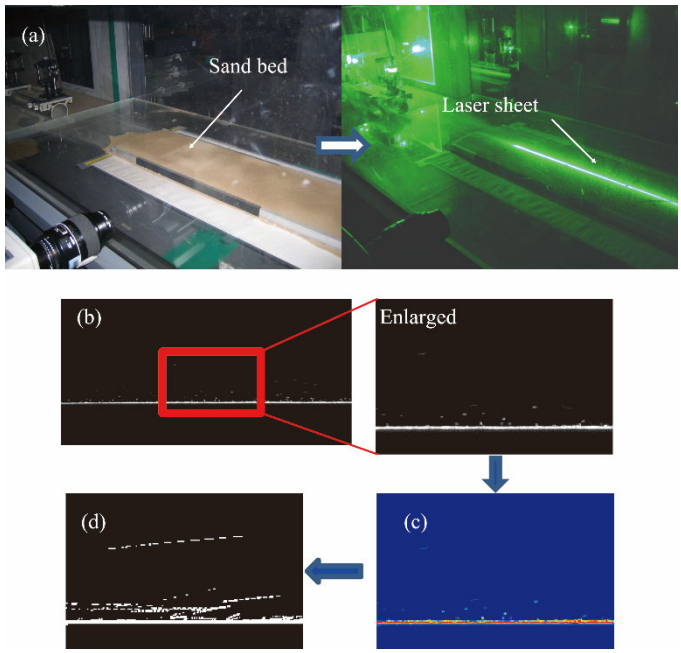

Fig. 2 Measurement of windblown sand flow in wind tunnel. (a), physical photo of the experimental setup; (b), one of the recorded particle image and its partially enlarged display; (c), recognition of the connected domains by dynamic threshold scheme. The dark blue represents the background, and the different colors represent the different levels of image segmentation; and (d), trajectory of sand particles.

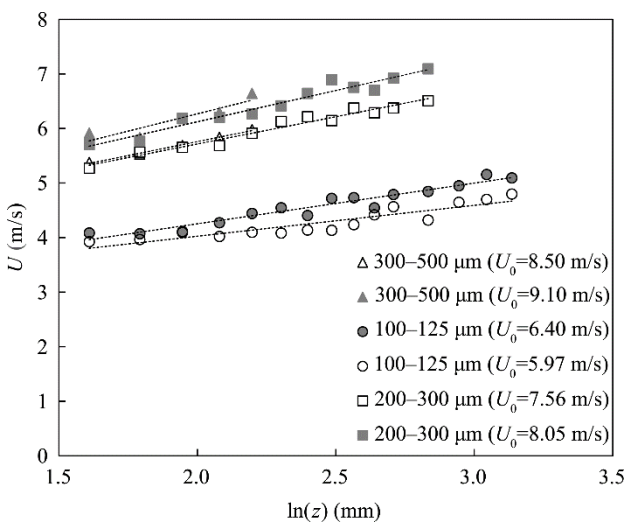

Fig. 3 Streamwise wind velocity (U) profiles. The dashed lines refer to the linear fittings of the relationship of U and ln(z).

The maximum height of the sand particles in each image is approximately the hop height of the saltons. Therefore, the average value of the maximum heights for all particle trajectories is defined as h_s. The average height for all moving sand particles is defined as h_m. These two kinds of height of moving sand particles versus the effective wind shear velocity are shown in Figure 4. To determine if the windblown sand flow has reached the steady state, each image is divided into two

equal parts along the flow direction, and the change rate (R) of moving sand particles is calculated as $R=(N_u-N_d)/(N_u+N_d)$, where N_u and N_d are the numbers of moving sand particles at the upstream and downstream parts of the region covered by the recorded image, respectively. When most of R is less than 0, it means that more and more sand particles are blown up as wind moves toward downstream, i.e., the sand flow does not reach the steady state. However, when R fluctuates around 0, it means that sand particles carried by wind reaches the dynamic equilibrium, i.e., the sand flow is in the steady state. In this case, the fluctuation of R results from the intermittent nature of sand flow (Platzer and Francois, 2011). The result of R is shown in Figure 5. As one can see, for each sand sample, the sand flow reaches the steady state only at the relatively low wind shear velocity. According to Figure 4, however, the hop height of saltons and the average height of all moving sand particles are related to the wind shear velocity only, thusly disregarding whether the sand flow is steady. Therefore, the unsaturated state does not affect the scaling law of launch velocity of sand particles.

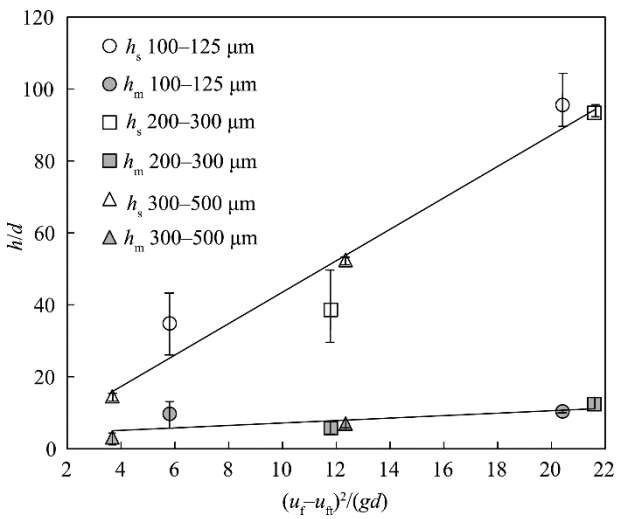

Fig. 4 Hop height of saltons and average height of moving sand particles versus the effective wind shear velocity. The height is normalized by mean diameter d, and the effective wind shear velocity squared is normalized by gd.

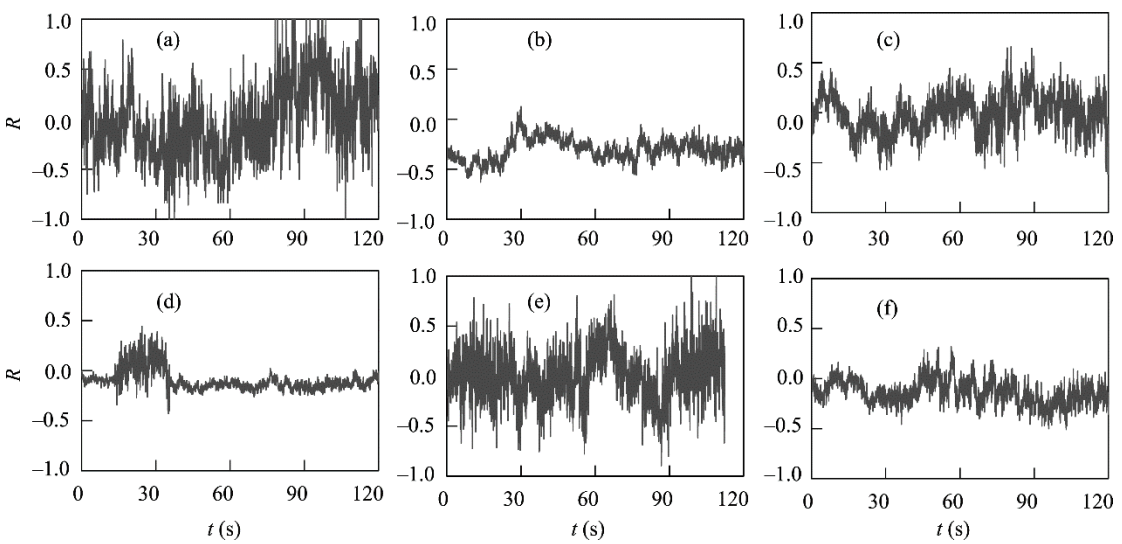

Fig. 5 Change rate (R) of the number of moving sand particles along the flow direction versus time. (a) and (b) are for the 100–125 μm sand with u_f=0.23 m/s and u_f=0.30 m/s, respectively. (c) and (d) are for the 200–300 μm sand with u_f=0.40 m/s and u_f=0.46 m/s, respectively. (e) and (f) are for the 300–500 μm sand with u_f=0.41 m/s and u_f=0.51 m/s, respectively.

According to the results shown in Figure 4, the relationship between the dimensionless hop height and effective shear velocity can be fitted linearly as

$$\begin{aligned} h_s / d &= 4.37(u_f - u_{ft})^2 / (gd) - 0.20 \\ h_m / d &= 0.34(u_f - u_{ft})^2 / (gd) + 3.74 \end{aligned} . \tag{9}$$

By comparing Equations 4 and 9, we can obtain c_s=1.48. The average height is

$$h_m / d = P h_{ms} / d + (1-P) h_{mr} / d , \tag{10}$$

where the average height of saltons h_{ms} equals to $0.5h_s$ because the heights of saltons in each image are assumed to be distributed evenly in the range of 0–h_s. Similarly, the average height of reptons h_{mr} is $0.5h_r$; P is the percentage of saltons among all moving sand particles and remains approximately constant because the explored range of u_f/u_{ft}, namely, 1.41–2.00, is narrow. h_m/d and h_s/d are linear functions of $(u_f–u_{ft})^2/(gd)$. According to Equation 10, the experimental result of h_r/d can be also fitted with a linear function, which is assumed as:

$$h_r / d = A(u_f - u_{ft})^2 / (gd) + B , \tag{11}$$

where A and B are unknown coefficients. By substituting Equations 9 and 11 into Equation 10, one can obtain the following relationship:

$$(0.68 - 4.37P - A(1-P))(u_f - u_{ft})^2 / (gd) + 7.48 + 0.20P - B(1-P) = 0 . \tag{12}$$

This equation should hold for all values of $(u_f–u_{ft})^2/(gd)$, that is:

$$\begin{aligned} 0.68 - 4.37P - A(1-P) &= 0 \\ 7.48 + 0.20P - B(1-P) &= 0 \end{aligned} . \tag{13}$$

The sand motion below the focus point is independent of wind shear velocity (Ho et al., 2014). Hence, A=0 according to Equation 11. Then, P=0.16 and B=8.94. The fitted line for the experimental result of h_r/d is h_r/d=8.94, which yields c_r=2.11 according to Equation 4. Therefore, $v_r=4.22(gd)^{1/2}$ and $v_s=2.96(u_f–u_{ft})$. As shown in Figure 4 and Equation 9, the slope of h_m/d versus the effective shear velocity squared is nearly zero and about ten times smaller than that of h_s/d; meanwhile, the slope of h_r/d is theoretically zero. That is to say, reptons contribute to the most of the average hop height. This is consistent with the fact that sand particle concentration decreases drastically (such as exponentially) as the height increases (Dong et al., 2003; Kang, 2012). By using a sand sample with a mean diameter of 230 μm, Ho et al. (2011) found that the average vertical launch velocity is $10.64(gd)^{1/2}$ over an erodible sand bed, whereas the average vertical launch velocity is $5.8(u_f–u_{ft})$ over a non-erodible sand bed. As discussed in Section 4, the majority

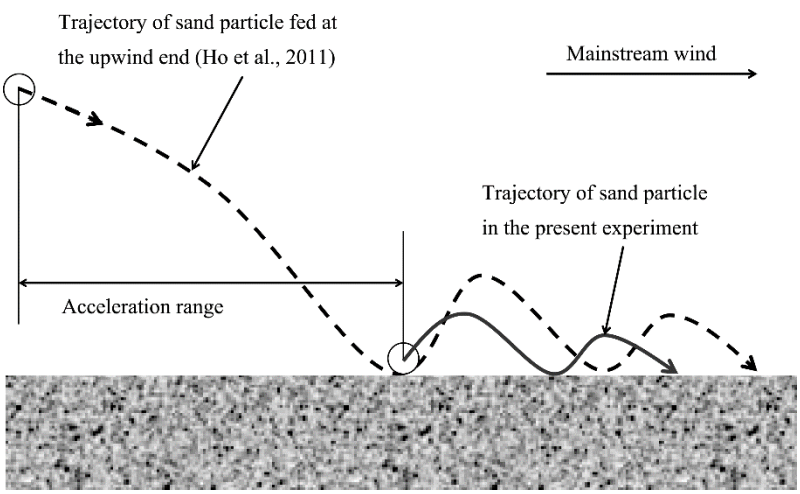

Fig. 6 Trajectories of sand particles on the flat sand bed. Compared to the grain in the present experiment, the grain in Ho et al. (2011) will experience an extra acceleration process before the first launch process.

of the moving sand particles are reptons for the erodible sand bed and are saltons for the non-erodible sand bed. Therefore, their scaling law is qualitatively the same as that of the present study, while their coefficients c_r (5.32) and c_s (2.90) are larger than the corresponding values in the present experiment. This is because the sand particles in their experiment was supplied at the upwind end of the wind tunnel, which resulted in an extra acceleration process before the first launch process (Fig. 6). As a result, the launch velocities as well as the hop lengths are larger than those in the present experiment. Above all, the scaling law in Equation 4 are consistent with the results extracted from Figure 4, the revisited scaling law are thusly considered reasonable.

4 Explanation of the discrepancies among the classical models

According to Equations 7 and 8, the dependence of q on u_f varies from quadratic to cubic as the ratio for particle number of saltons to reptons increases. These scaling law is used to explain the discrepancies among the classical models of q shown in Table 1. In a word, the scaling law of q depends on the ratio of saltons number to reptons number. For a small u_f over erodible sand beds, reptons account for the majority of moving particles, leading to a quadratic dependence of q on u_f according to Equation 7, which agrees with the results of Creyssels et al. (2009) and Ho et al. (2011) for erodible sand beds, Durán et al. (2011) for small u_f, and Martin and Kok (2017) for a large u_f over erodible sand beds or for non-erodible sand beds where the height of the focus point is only d/30, saltons are the majority. Therefore, the dependence of q on u_f should be cubic according to Equation 8, thereby supporting the results of Durán et al. (2011) for large u_f and Ho et al. (2011) for non-erodible sand beds. The dependence of q on u_f, which varies from quadratic to cubic (Sauermann et al. 2001), is caused by the increase in the ratio of saltons to reptons. The cubic scaling law for q in Bagnold (1941) and Kind (1976) was obtained by assuming that the vertical launch velocity scales uniformly with u_f. However, this assumption is unconvincing because the vertical launch velocity of reptons is independent of u_f.

The cubic scaling law for q in subaquatic cases can be understood in the same way. In windblown sediment transport, the wind velocity profile is logarithmic above the focus point and is independent of u_f below the focus point (Ho et al., 2014). By contrast, the fluid velocity profile is logarithmic throughout the boundary layer (Lajeunesse et al., 2010). As a result, water-driven sand flows have no focus point, that is, the height of the focus point is zero. Therefore, all moving sand particles can be viewed as saltons, leading to a cubic scaling law for q.

Table 1 Models for the steady sand transport rate

Reference	Expression	u_f/u_{ft}
Bagnold (1941)	$q \propto (d/d_0)^{1/2}\rho u_f^3$	-
Kind (1976)	$q \propto \rho u_f(u_f^2-u_{ft}^2)/g$	-
Creyssels et al. (2009)	$q \propto \rho(u_f^2-u_{ft}^2)(d/g)^{1/2}$	≤3.4
Martin and Kok (2017)	$q \propto \rho(u_f^2-u_{ft}^2)(d/g)^{1/2}$	≤2.2
Sauermann et al. (2001)	$q \propto u_f^n$, $n \in (2, 3)$	-
Ho et al. (2011)	$q \propto \rho(u_f^2-u_{ft}^2)(d/g)^{1/2}$ for erodible bed	-
	$q \propto \rho(u_f-u_{ft})(u_f^2-u_{ft}^2)/g$ for non-erodible bed	-
Durán et al. (2011)	$q \propto \rho u_f(u_f^2-u_{ft}^2)/g$ at large u_f	-
	$q \propto \rho(u_f^2-u_{ft}^2)(d/g)^{1/2}$ at small u_f	-

Note: d_0=250 μm is the reference sand diameter. Sauermann et al. (2001) suggested that q is proportional to u_f^n, where n increases from 2 to 3 as the wind shear velocity increases. -, no data available.

5 Conclusions

By incorporating a dimensional analysis and a wind tunnel experiment, the present work shows that the ratio of saltons number to reptons number determines the scaling law of sand particle launch velocity and steady sand transport rate. When saltons account for the majority of moving sand particles, the average launch velocity depends on wind shear velocity, and the steady sand transport

rate scales with the cubic of wind shear velocity; when reptons take the majority, the average launch velocity is independent of wind shear velocity, and the steady sand transport rate scales with the quadratic of wind shear velocity. This conclusion provides a succinct framework in which the differences among the previous experimental results can be interpreted. Furthermore, for a moderate shear velocity, reptons take the majority of moving sand grains for aeolian transport. Then according to the formula of hop length $l_r \propto d$, one can infer that in aeolian transport the larger the sand size is, the farther the sand jumps. This might be the reason for the sand sieving phenomenon: a greater fraction of large grains is observed as the distance to the wind tunnel entrance increases (Durán et al., 2011). The next step is to investigate a more effective way of monitoring the temporal-variant ratio of saltons to reptons under a wide range of wind velocity, so that the windblown sand transport can be correctly quantified under various circumstances, and the critical velocity at which the scaling law switches can be distinguished.

Acknowledgements

This work is funded by the National Natural Science Foundation of China (11402190), the China Postdoctoral Science foundation (2014M552443) and the Shaanxi Province Natural Science Foundation Research Project (2018JM1021).

References

Anderson R S, Hallet B. 1986. Sediment transport by wind: toward a general model. Geological Society of America Bulletin, 97(5): 523–535.

Andreotti B, Claudin P, Douady S. 2002. Selection of dune shapes and velocities. Part 1: Dynamics of sand, wind and barchans. The European Physical Journal B, 28(3): 321–339.

Bagnold R A. 1941. The physics of blown sand and desert dunes. Nature, 18: 167–187.

Bagnold R A. 1973. The nature of saltation and of 'bed-load' transport in water. Proceedings of the Royal Society of London Series A-Mathematical Physical and Engineering Sciences, 332: 473–504.

Burr D M, Bridges N T, Marshall J R, et al. 2015. Higher-than-predicted saltation threshold wind speeds on Titan. Nature, 517: 60–63.

Creyssels M, Dupont P, El Moctar A O, et al. 2009. Saltating particles in a turbulent boundary layer: experiment and theory. Journal of Fluid Mechanics, 625: 47–74.

Dong Z B, Wang H T, Zhang X H, et al. 2003. Height profile of particle concentration in an aeolian saltating cloud: a wind tunnel investigation by PIV MSD. Geophysical Research Letter, 30(19): 153–166.

Durán O, Claudin P, Andreotti B. 2011. On aeolian transport: Grain-scale interactions, dynamical mechanisms and scaling laws. Aeolian Research, 3(3): 243–270.

Feng D J, Li Z S, Ni J R. 2009. Launch velocity characteristics of non-uniform sand in windblown saltation. Physica A: Statistical Mechanics and Its Applications, 388(8): 1367–1374.

Ho T D, Valance A, Dupont B P, et al. 2011. Scaling laws in aeolian sand transport. Physical Review Letters, 106(9): 094501.

Ho T D, Valance A, Dupont B P, et al. 2014. Aeolian sand transport: Length and height distributions of saltation trajectories. Aeolian Research, 12: 65–74.

Kang L Q. 2012. Discrete particle model of aeolian sand transport: comparison of 2D and 2.5D simulations. Geomorphology, 139–140: 536–544.

Kind R J. 1976. A critical examination of the requirements of model simulation of wind induced erosion/deposition phenomena such as snow drifting. Atmospheric Environment, 10(3): 219–227.

Kok J F, Parteli E J R, Michaels T I, et al. 2012. The physics of wind-blown sand and dust. Reports on Progress in Physics, 75(10): 106901.

Lajeunesse E, Malverti L, Charru F. 2010. Bed load transport in turbulent flow at the grain scale: experiments and modeling. Journal of Geophysical Research, 115(F4): 745–751.

Martin R L, Kok J F. 2017. Wind-invariant saltation heights imply linear scaling of aeolian saltation flux with shear stress. Science Advances, 3(6): e1602569.

Mcewan I K, Willetts B B. 1993. Adaptation of the near-surface wind to the development of sand transport. Journal of Fluid Mechanics, 252: 99–115.

Namikas S L. 2003. Field measurement and numerical modelling of aeolian mass flux distributions on a sandy beach. Sedimentology, 50: 303–326.

O'Brien P, McKenna Neuman C. 2016. PTV measurement of the spanwise component of aeolian transport in steady state. Aeolian Research, 20: 126–138.

O'Brien P, McKenna Neuman C. 2018. An experimental study of the dynamics of saltation within a three dimensional framework. Aeolian Research, 31: 62–71.

Ohmi K, Li H Y. 2000. Particle-tracking velocimetry with new algorithms. Measurement Science and Technology, 11(6): 603–616.

Owen P R. 1964. Saltation of uniform grains in air. Journal of Fluid Mechanics, 20(2): 225–242.

Platzer B. François Charru. 2011. Hydrodynamic Instabilities (translated by Patricia de Forcrand-Millard). Cambridge, Cambridge University Press.

Rasmussen K R, Sørensen M. 2008. Vertical variation of particle speed and flux density in aeolian saltation: Measurement and modeling. Journal of Geophysical Research, 113(F2): 544–548.

Sauermann G, Kroy K, Herrmann H J. 2001. Continuum saltation model for sand dunes. Physical Review E, 64: 031305.

Sørensen M. 2004. On the rate of aeolian sand transport. Geomorphology, 59(1–4): 53–62.

Tennekes H, Lumley J L. 1972. A First Course in Turbulence. Cambridge, the MIT Press, 5.

Wang Y, Wang D W, Wang L, et al. 2009. Measurement of sand creep on a flat sand bed using a high speed digital camera. Sedimentology, 56(6): 1705–1712.

Wu W, Yan P, Wang Y, et al. 2018. Wind tunnel experiments on dust emissions from different landform types. Journal of Arid Land, 10(4): 548–560.

Yang B, Wang Y, Zhang Y. 2009. The 3-D spread of saltation sand over a flat bed surface in aeolian sand transport. Advanced Powder Technology, 20(4): 303–309.

Zhang W, Kang J H, Lee S L. 2007. Tracking of saltating sand trajectories over a flat surface embedded in an atmospheric boundary layer. Geomorphology, 86(3–4): 320–331.

Zhang W, Wang Y, Lee S J. 2008. Simultaneous PIV and PTV measurements of wind and sand particle velocities. Experiments in Fluids, 45(2): 241–256.

Zhang Y, Wang Y, Jia P. 2014. Measuring the kinetic parameters of saltating sand grains using a high-speed digital camera. Science China: Physics, Mechanics & Astronomy, 57(6): 1137–1143.

Zhang Y, Wang Y, Yang B, et al. 2015. A particle tracking velocimetry algorithm based on the Voronoi diagram. Measurement Science and Technology, 26(7): 075302.

Zhang Y, Wang Y, Yang B, et al. 2016. Measurement of sand creep on a flat sand bed using a high-speed digital camera: Mesoscopic features of creeping grains. Sedimentology, 63(3): 629–644.